J. Mater. Environ. Sci. 4 (5) (2013) 786-791
ISSN : 2028-2508
CODEN: JMESCN

Corrosion of P235GH carbon steel in simulated Bure soil solution

Y. El Mendili[1*], A. Abdelouas[1], J.-F. Bardeau[2]

[1] *SUBATECH, CNRS-IN2P3, Ecole des Mines de Nantes-Université de Nantes, 4 rue Alfred Kastler, BP 20722, 44307 Nantes cedex 03, France*

[2] *LUNAM Université, Institut des Molécules et Matériaux du Mans, UMR CNRS 6283, Université du Maine, Avenue Olivier Messiaen, 72085 Le Mans Cedex 9, France*

Received 29 Mars 2013, Revised 13 May 2013, Accepted 13 May 2013
* Corresponding author. E mail: elmendil@subatech.in2p3.fr; Tel : +33-2 51 85 86 35.

Abstract
In this study, the corrosion of carbon steel in the presence of Callovo-Oxfordian (COx) claystone/groundwater, was investigated. To more closely emulate the storage conditions, the corrosion tests were systematically conducted under controlled atmosphere of 5% H_2/N_2, at different temperatures (three months at 30°C followed by three months at 90° C with COx claystone and synthetic groundwater. The corrosion products formed on the steel surface have been studied by Scanning Electron Microscope/Energy Dispersive X-ray Spectroscopy and confocal micro-Raman measurements. Chemical analyses have been performed by Inductively Coupled Plasma with Mass Spectrometry and ionic chromatography. At 30°C, the iron release in solution allowed the appearance of magnetite phase followed by the transformation of magnetite into mackinawite. However, the pyrite phase was formed when the temperature of 90 ° C was reached. The appearance of pyrite in the corrosion system at 90°C testifies in most cases that the transition phase from mackinawite to pyrite was influenced by both temperature and the excess of sulphide ions produced by sulphate-reducing-bacteria metabolism.

Keywords: Carbon steel, SEM, Raman spectroscopy, effect of temperature, Microbiological corrosion.

Introduction
One of the French options for the final disposal of high-level radioactive waste is a deep geological repository. Geological disposal is based on the principle that the deep rock environment is stable and largely unaffected by environmental change for hundreds of thousands – even millions of years. Materials that are carefully emplaced deep underground will be well isolated from people and the environment in which we live. On the basis of different repository concepts, different host rocks have been examined in many countries for a number of years for their suitability to host a repository for high-level radioactive and heat-generating waste. For the selection of a possible repository site, the geological conditions play an essential role. In France, the Callovo-Oxfordian formation in the Meuse and Haute-Marne (Bure) was proposed to be the site of an underground research laboratory in order to evaluate in situ the interaction between the host formation and the engineered barriers. One of the most important criteria for the safety assessment concerns the life time of metal containers. In this deep environment (elevated pressure and temperature, low water content) many factors may induce a corrosion of metal containers (carbon steel). Moreover, since the discovery of micro-organisms in the Callovo Oxfordian clayey environment [1], a new corrosion parameter 'biocorrosion process' must also be taken into account and has to be investigated to improve the geochemical prediction on the sustainability of containers in geological disposal. Indeed, in recent study, El Hajj et al. [2] found that the COx claystone showed the presence of four strains from the spore-forming genera: *Desulfosporosinus*, *Desulfotomaculum*, *Thermosubterraneum* and *Desulfotomaculum* sp175. These groups of bacteria are known for their resistance to extreme conditions of temperature, pressure and lack of nutrients.
In this paper, we studied the role of the temperature increase in disposal site following sealing of galleries on microbiological viability. The temperature is expected to reach about 90°C a few decades after site closure due to radioactive decay of heat generating waste such as ^{137}Cs.The aim of this investigation was to identify the structural properties of the corrosion layer formed on the carbon steel surface under geological conditions from one to three months at 30°C and from three to six months at 90°C, in the presence of COx claystone.

2. Materials and methods
2.1. The COx claystone preparation
The claystone used was obtained from extracted COx argillite originating from Bure site (East of France) at a depth of about 490 m. COx argillite contains 40%–45% clay minerals (illite-smectite interstratified minerals being the

dominant clay minerals), 20%–30% carbonates, and 20%–30% quartz and feldspar [3,4]. The obtained COx argillite was then air-dried and crushed to powder.
The synthetic water composition in equilibrium with the claystone was prepared according to a procedure described by BRGM [5]. This synthetic groundwater is prepared by mixing the following reagents: $NaHCO_3$, Na_2SO_4, Na_2SiO_3, NaCl, KCl, $CaCl_2.2H_2O$, $MgCl_2$ $6H_2O$, $SrCl.6H_2O$. The solution was bubbled with a mixture of Ar/CO_2. The final composition of the synthetic water is presented in Table 1.

Table 1: Chemical composition of the synthetic groundwater.

		Concentrations (mmol/L)										
pH	pe	Al	Fe	Si	Sr	K	Mg	Ca	Na	Cl	S(VI)	S(-II)
7.2	-3.0	$6.3\ 10^{-6}$	0.047	0.18	0.21	1.04	5.4	8.5	43.2	41.0	14.7	$4.0\ 10^{-7}$

2.2. The steel preparation
The P235GH carbon steel was used in these experiments because it is a heat-resistant pressure-vessel steel, characterized by a good weldability. It is used above all for manufacturing boilers, pressure vessel and pipes transporting hot liquids. In disposal conditions, the carbon steel overpacks are intended to last for a few thousands of years to prevent glass alteration while temperatures become high (50-90°C) and radionuclides release in the surrounding environment.
The steel coupons were cut into 10 × 10 × 1 mm pieces, polished with a Buehler polisher using a PSA disc (Pressure Sensitive Adhesive discs) to a surface roughness of 3 µm and cleaned with HCl (15%) + $NaCO_3$ (5%) solution as described in the ASTM standard method for corrosion measurement. [6] The polished samples were then ultrasonically cleaned with ethanol for 1 min, degreased with acetone, air-dried, and stored under vacuum before experiments.

2.2. The sample preparation
Steel coupons were corroded in claystone/COx water batch cultures. The experiments were conducted in serum bottles with four steel coupons (two for mass loss and two for the structural characterization) mixed with 20 g of COx claystone and 100 ml of synthetic groundwater. Lactate was added to groundwater to emulate the growth of sulphate-reducing-bacteria (SRB) from claystone.
The experiments were conducted at 30 °C for 3 months before continuing at 90 °C for three more months, under strictly anaerobic conditions in serum bottles and under an atmosphere of 5% H_2/N_2 (0.25 bar) to prevent oxygen contamination and to simulate reducing conditions that will be encountered in the expected Bure disposal site.

2.4. Weight loss measurements
For all experiments, the corrosion rate of carbon steel was determined by gravimetric method. The corrosion layer was pickled with HCl (15%) and isopropanol with 5mg/l of hexamethylene tetramine to inhibit corrosion.
The corrosion rate of metal was determined using the following equation:

Corrosion rate micron/year: $$V_{cor}(\mu m/year) = \frac{3650 \text{ x weight loss (mg)}}{\text{Density (g/cm}^3\text{) x Area (cm}^2\text{) x Time (days)}}$$

With a density of 7.85 g/cm³ for steel

2.4. Chemical and surface analysis
At the end of reaction time, an aliquot of the solution was syringe-filtered using a 0.2 µm polypropylene filter (Whatman). The solution was then analyzed by Inductively Coupled Plasma-Mass Spectrometry (ICP-MS, Perkin-Elmer) to quantitatively determine the iron concentration. Sulphide concentration was measured by UV-VIS spectroscopy (UV-2401 PC Shimadzu) at 665 nm.
The surface morphology of the corroded coupons after immersion was examined by Scanning Electron Microscopy (SEM, JEOL 6400LV). The chemical composition of the layer formed on the steel surface was determined by Energy Dispersive X-ray analysis (EDX) coupled to the SEM. The analyses were done with an accelerating voltage of 15 kV.
The identification of the corrosion products and phases was achieved using confocal micro-Raman analysis. The Raman experiments were carried out using a Horiba Jobin-Yvon T64000 spectrometer equipped with a 600 lines mm^{-1} grating coupled to a liquid-N_2-cooled charge-coupled device detector. Raman spectra were recorded at room temperature in backscattering configuration under a microscope (Olympus Bx41) with a 100x objective focusing the 514.5 nm line from an Argon-Krypton ion laser. The spot size of the laser was estimated at 0.8 µm and the spectral resolution at 2 cm^{-1}. Raman measurements were carried out at very low laser power (0.8 mW) to avoid structural

modifications or phases transitions [7]. Single spectra were recorded twice in the wavenumber 100-1500 cm^{-1} region with an integration time varying between 400 s and 600 s. The Raman spectra were analysed using Labspec v5.25 software.

3. Results and discussion

3.1. SEM analysis

Morphology observation and elemental analysis of corrosion products formed on steel surface are presented in Figure 1. In the first month, the steel is covered with a gray layer mainly made of iron and oxygen suggesting the formation of iron oxides (Fig. 1a). Microanalysis performed on the steel coupons shows that the main elements in the surface are Fe and O. The elemental composition (in weight %) of Fe and O were 42% and 54%, respectively. This indicates that Fe has reacted with O from the medium (H_2O) to form iron oxide as a corrosion product. The concentrations of iron and oxygen correspond to the stoichiometry of magnetite Fe_3O_4. The iron and oxygen are accompanied by the presence of Si, Al, Na, Mg,… originating from the synthetic water and claystone, in mass quantities of less than a few percents. At 3 and 6 months (Fig. 1b-1c), the steel coupons turned all black and the SEM image shows the presence of a uniform layer on the entire surface. EDX analysis revealed the presence of sulphur and iron, suggesting a formation of iron sulphide. We also noted that the concentration of sulphur significantly increases between the 3rd and 6th month.

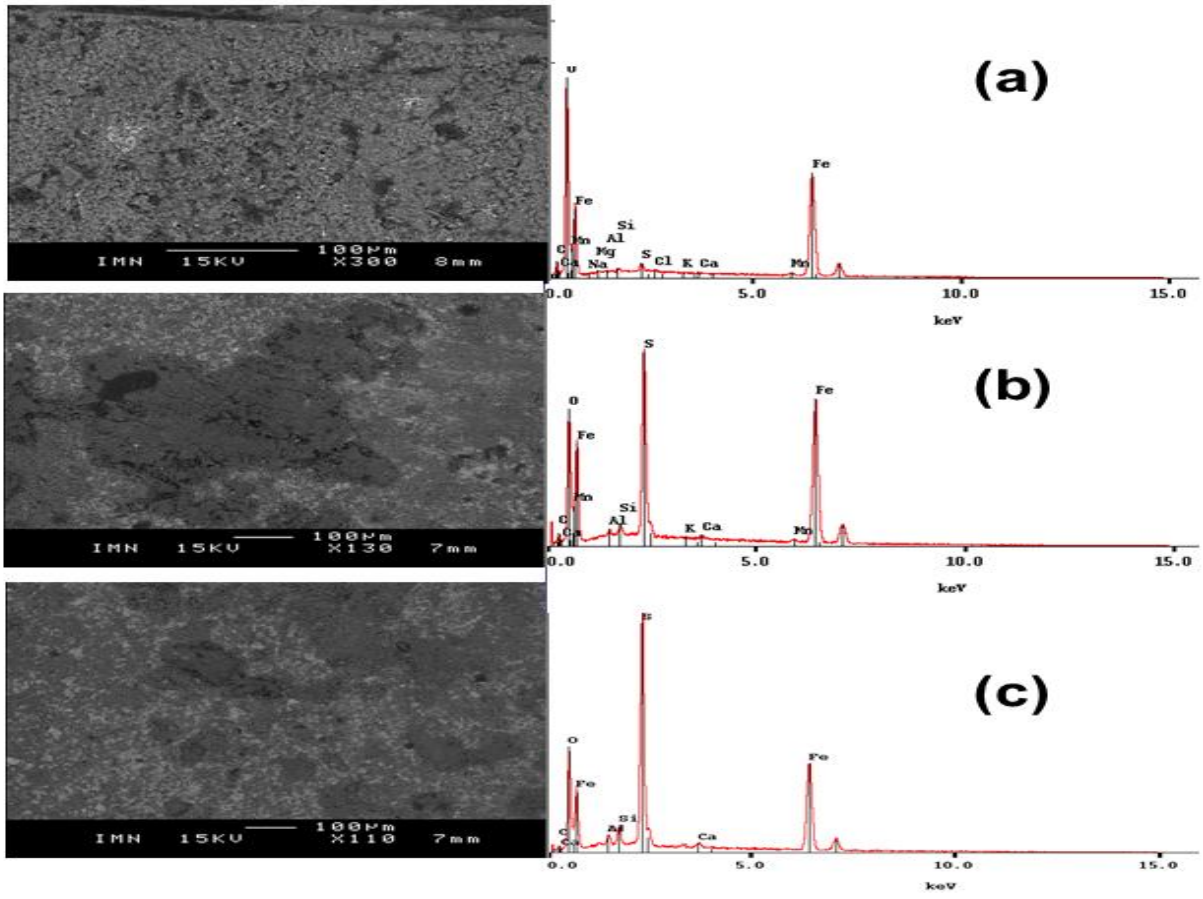

Figure 1: SEM photographs of the steel surface of different systems with the corresponding chemical microanalysis spectra. a) After 1 month, b) 3 months and c) 6 months.

3.2. Raman investigation

The Raman spectra recorded on steel coupons under anaerobic condition and after different incubation time are presented in figure 2. After 1 month of incubation at 30°C, Raman spectrometry analysis of the steel surface essentially shows the presence of magnetite. Indeed the Raman spectrum shows the five predicted Raman bands for magnetite phase [8]: A_{1g} at 668 cm^{-1}, E_g at 306 cm^{-1}, and T_{2g} at 538, 193, and ~ 450 cm^{-1}. At higher wavenumber (~ 1378 cm^{-1}), there are no apparent peak. Hence, this result gives the obvious evidence for the existence of Fe_3O_4 other than γ-Fe_2O_3. [9]. After 2 months of incubation at 30°C, the corresponding Raman spectrum shows the presence of two peaks around 209 cm^{-1} and 282 cm^{-1}. These vibrations were also attributed to poorly crystallized iron sulphide [10] present in the corrosion products of non-alloy steel in the presence of H_2S or in sediments. The bands at 282 cm^{-1}

and 208 cm^{-1} are attributed to the symmetric stretching mode of FeS and to the lattice mode respectively. The Raman spectrum obtained after 3 months is slightly different from that obtained at room temperature. It consists of four peaks with the two main peaks at 209 and 286 cm^{-1} corresponding to poorly crystallized iron sulphide and four broad peaks at 255, 310, 360 and 475 cm^{-1}. The mode at 475 cm^{-1} is probably due to elemental sulphur [11]. The other modes have been attributed in the literature to mackinawite ($Fe_{1+x}S$). [12] Even though, no Raman band assignment was given by these authors. It has been evidenced that the mechanism through which SRB could act involves the formation of hydrogen sulfide with the precipitation of iron sulfide and the formation of elemental sulfur [13].

The transfer of steel coupons from 30°C that lasted for 3 months to 90°C for 3 months shows the formation of pyrite in steel surface. Indeed, the spectrum shows the main Raman bands: A_g (379 cm^{-1}), E_g (343 cm^{-1}) and T_g (430 cm^{-1}) [14,15] characteristic of pyrite. Accordingly, our Raman investigations clearly reveal the crystallization of poorly crystallized iron sulphide into mackinawite at 30°C, followed by the phase transition from mackinawite to pyrite after the transfer of steel coupons to high temperature.

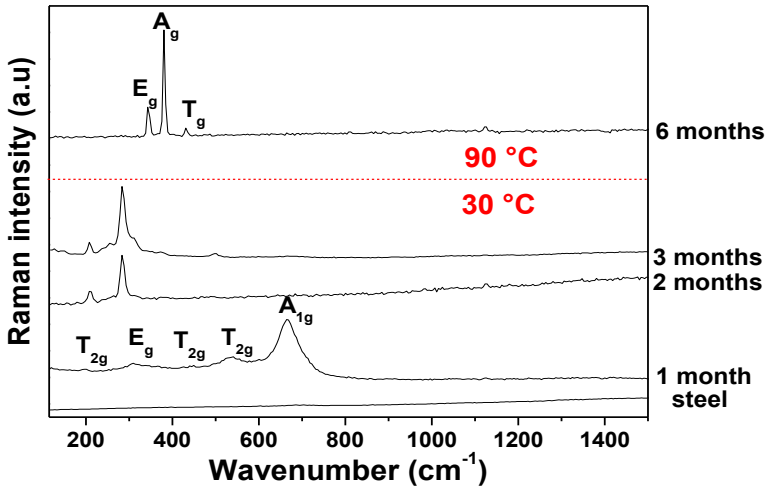

Figure 2: Raman spectra of steel coupons corroded under anaerobic condition as a function of incubation time.

3.3. Solution analysis

The evolution of iron and sulphide concentrations as a function of time exposure is presented in figure 3. We note a similar behavior of Fe^{2+} and S^{2-} concentrations in solution. It should be noted that the iron at the beginning of the experiment is due to its presence in synthetic groundwater.

The concentration increase of sulphide ions (S^{2-}) until the 2nd month is due to the formation of (H_2S) produced by SRB metabolism. The increase of Fe concentration is related to the dissolution of iron. In this scenario, the metal will be corroded and eventually lead to significant structural damage. The decrease of Fe concentration starting from 2 months is due to sulphide precipitation with the Fe^{2+} ion to form iron sulphide.

The amount of Fe^{2+} and H_2S have an immense influence on the formation and protective ability of the iron sulfide formed [16]. Increasing Fe^{2+} concentration can lead to higher super saturation of iron sulphide, which could increase the precipitation rate of iron sulphide (between 1 and 3 months). The precipitated film could be very protective by being dense and acting as a diffusion barrier to the corrosive species, or it could be porous and thick and still could not be protective. Hence, crystallinity of the film is the most important factor in determining the corrosion rate of the film.

Recently, Ma et al. [17] found that H_2S can either accelerate or inhibit corrosion of iron under different experimental conditions such as H_2S concentration and solution pH. The inhibition effect is attributed to the formation of iron sulphide protective film for H_2S at high concentrations of H_2S. When the test conditions are favorable for the formation of different types of protective iron sulphide films, higher temperature may help facilitate the film formation, as is the case in our study with the formation of more protective iron sulphide 'pyrite'. In addition, pyrite has a lower solubility than the poorly-crystallised and nearly amorphous mackinawite. Indeed, for instance, the solubility of iron sulfides at 25°C and 1.8 MPa pressure are in the ratio 6000:1 for mackinawite and pyrite respectively [18]. Compared with other iron sulfides, the mackinawite is the most soluble and has the highest dissolution rate. Consequently, converting the carbon steel surface layers to pyrite will give minimum iron transport and thus maintaining low Fe concentration in solution.

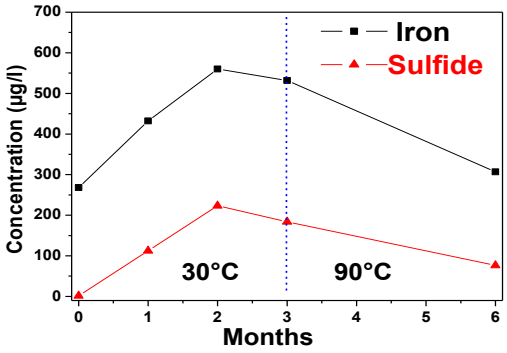

Figure 3: Evolution of iron and sulphide concentrations of solution as a function of time.

3.3. Corrosion rate

The results of corrosion rate derived from weight loss are plotted in Figure 4. The coupon surface which was in contact with sulphide-rich water (after 1 month) was significantly blackened after exposure due to the formation of iron sulphide. The corrosion rate rapidly increases up to 3 months and remains nearly constant between 2 and 3 months. The transfer of steel coupons from 30°C that lasted for 3 months to 90°C for 3 months lead to the decrease in corrosion rate, indicating that high concentrations of sulphide inhibit the corrosion reaction by pyrite formation.

It is observed that the corrosion rate of steel coupon was affected by the structural properties, density and the stability of iron sulphide formed [16]. Indeed, when a crystal structure is converted into a denser structure, an adherence of the corrosion layer is expected. It is worth noting that pyrite is of significantly higher density than mackinawite, 4.84 g/cm^3 versus 4.29g/cm^3.

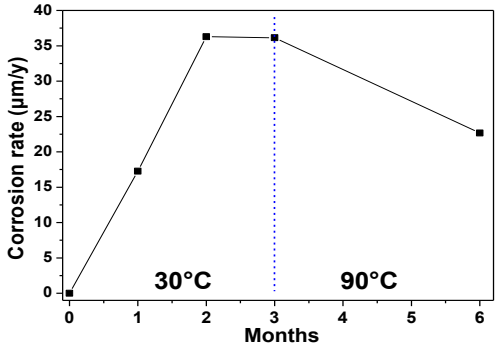

Figure 4: Evolution of corrosion rate as function of time aging.

In the first step of anaerobic environment, the first corrosion products are mainly ferric iron(II) hydroxide ($Fe(OH)_2$) and magnetite (Fe_3O_4) with generally low steel corrosion rates <10 µm/y [19,20]. The reactions are:

Reduction of water: $2H_2O + 2e^- \rightarrow H_{2(g)} + 2OH^-$ (1)

Oxidation of iron: $Fe_{(s)} + 2OH^- \rightarrow Fe(OH)_{2(s)} + 2e^-$ (2)

Hence the global reaction is: $Fe_{(s)} + 2H_2O \rightarrow Fe(OH)_{2(s)} + H_{2(g)}$ (3)

$Fe(OH)_2$ (s) formed is transformed into magnetite:

$3Fe(OH)_{2(s)} \rightarrow Fe_3O_{4(s)} + H_{2(g)} + 2H_2O$ (4)

The corrosion of steel produces hydrogen which diffuses into the water. The SRB with their hydrogenase activity, use hydrogen produced by the reduction of the proton to reduce sulfate SO_4^{2-} into hydrogen sulphide H_2S.

SRB metabolize as follows: $4H_2+SO_4^{2-}+2H^+ \rightarrow 4H_2O+ H_2S$ (5)

The iron oxide transformation into iron sulphide under the presence of hydrogen sulphide provided by SRB sulphate reduction is given by [21]:

$Fe_3O_4 + H_2S \rightarrow 3\ FeS + S + 4\ H_2O$ (6)

The final product is FeS_2, or pyrite, which is a nonreactive and relatively stable compound.

$FeS + S = FeS_2$ (7)

Several studies have shown the formation of a variety of iron sulphide such as mackinawite ($Fe_{1+x}S$), pyrrhotite ($Fe_{1-x}S$), monoclinic troilite (FeS) and pyrite depending of the environmental conditions [22-27]. The formation of the mackinawite has been established in aqueous media with a formation mechanism involving a solid

transformation of magnetite in contact with aqueous sulphide [23,24]. Pyrite formation is found in a variety of natural environments such as marine sediments swamps and soils [25-27]. It is becoming increasingly clear that in our case the sulfate-reducing bacteria play an important role by providing hydrogen sulfide and the temperature accelerates the transformations of mackinawite into pyrite.

With exposure time and the excess of sulfide, the composition of the protective layer formed of iron sulphide transformed from mackinawite to pyrite. The corrosion films formed after 6 months at 90°C exhibited more protective properties. The enhanced protection is then attributed to the transformation of nanocrystalline mackinawite into pyrite. Pyrite exhibits greater stability and more protective properties.

Conclusion

The present work shows that the corrosion rate of carbon steel under geological condition is affected by the structural properties of the corrosion products formed in the steel surface. The increase of sulphide concentration led to the formation of the more stable iron sulphide 'pyrite'. Our results show that the inhibition effect of sulphide on the carbon steel corrosion is attributed to the formation of pyrite protective film on the steel surface. The pyrite layer slows down the corrosion process by presenting a diffusion barrier for the species involved in the corrosion process and by covering and preventing the underlying steel from further dissolution.

Acknowledgements-This research has been supported by ANDRA (French National Radioactive Waste Management Agency).

References

1. Poulain S., Caractérisation microbiologique de l'argile à Opalinus du Mont Terri et de l'argilite du Callovo-Oxfordien de Meuse/Haute-Marne. Thèse, (2006).
2. El Hajj H., Abdelouas A., Grambow B., Martin C., Dion M. *Phys. Chem. Earth.* 35 (2010) 248.
3. ANDRA, Référentiel géologique du site de Meuse/Haute-Marne. Tome 1. Report No. C RP ADS. 2005b, 04-0022.
4. Zhang C. L, Rothfuchs T. *Appl. Clay. Sci.* 26 (2004) 325.
5. Tournassat C., Blanc P., Gaucher E., Estimation de la composition de l'eau porale du Callovo-Oxfordien à 50, 70, 80 et 90 °C, BRGM/RP-56171-FR. (2008).
6. ASTM Standards. Coupon test method D 2328-65 T. ASTM international standards worldwide. (1966).
7. El Mendili Y., Bardeau J.-F., Randrianantoandro N., Grasset F., Greneche J.-M. *J. Phys. Chem. C.* 116 (2012) 23785.
8. White W.B., DeAngelis B.A., *Spectrochimica Acta* 23A (1967) 985.
9. De Faria D. L. A., Silva S. V., de Oliveira M. T. *J. Raman. Spectrosc.* 28 (1997) 873.
10. Hansson E.B., Odziemkowski M.S., Gillham R.W. *Corros.Sci* .48 (2006) 3767.
11. Mycroft J.R., Bancroft G.M., McIntyre N.S., Lorimer J.W., Hill I.R. *J. Electroanal.Chem*. 292 (1990) 139
12. Bourdoiseau J.A., Jeannin M., Sabot R., Rémazeilles C., Refait P. *Corros. Sci.* 50 (2008) 3247.
13. Jones D.A., Amy P.S. *Corrosion* 58 (2002) 638–645.
14. Pisapia C., Chaussidon M., Mustin C., Humbert B. *Geochim. Cosmochim. Acta* 71 (2007) 2474.
15. Toniazzo V., Mustin C., Portal J.M., Humbert B., Benoit R., Erre R. *Appl. Surf. Sci.* 143 (1999) 229.
16. Sun W., Nesic S. NACE International Corrosion Conference & Expo, Paper No.06644, (2006).
17. Ma H., Cheng X.L., Li G.Q., Chen S.H., Quan Z.L., Zhao S.Y., Niu L. *Corros. Sci.* 42 (2000) 1669.
18. P.H. Tewari, G. Wallace, B. Allan Campbell, The Solubility of Iron Sulfides and Their Role in Mass Transport in Firdler-sulfide Heavy Water Plants, Research Chemistry Branch, Whiteshell Nuclear Research Establishment, (1978)
19. Jack T.R., Wilmott M.J., Sutherby R.L., Worthingham R.G. *Mater. Perf.* 35 (1996) 18.
20. Jack T.R., Wilmott M.J., Sutherby R.L. *Mater. Perf.* 34 (1995) 19.
21. Robert M., Berthelin J., Soil Science Society of America, Madison, Special Publication 17 (1986) 453.
22. Muronwich J. B., Barnes H. L. *Am. Mineral.* 71 (1986) 1243–1246.
23. Shoesmith D.W., Bailey M.G., Ikeda B. *Electrochim. Acta* 23 (1978) 1329.
24. Shoesmith D.W., Taylor P., Bailey M.G., Owen D.G. *J. Electrochem. Soc.* 127 (1980) 1007.
25. Gagnon C., Mucci A., Pelletier E. *Geochim. Cosmochim. Acta* 59 (1995) 2663.
26. Dellwig O., Bottcher M.E., Lipinski M., Brumsack H.J. Chem. Geol. 182 (2002) 423.
27. Brennan E.W., Lindsay W.L. *Geochim. Cosmochim. Acta* 60 (1996) 3609.